Design, prototyping and test of a Dual-Arm Continuum Robot for underwater environments

1st Nan Ma
Department of Engineering
Lancaster University
Lancaster, United Kingdom
n.ma1@lancaster.ac.uk

2nd Stephen Monk
Department of Engineering
Lancaster University
Lancaster, United Kingdom
s.monk@lancaster.ac.uk

3rd David Cheneler
Department of Engineering
Lancaster University
Lancaster, United Kingdom
d.cheneler@lancaster.ac.uk

***Abstract*—The decommissioning of nuclear sites is a significant and growing engineering challenge often requiring specialist equipment, especially when the nuclear site is partially submerged with contaminated water. However, most currently available decommissioning tools are large, bulky structures that lack dexterity. In this paper, a novel dual-arm continuum robot, which is composed of two 6-degree of freedom (DoF) continuum arms that can be simultaneously employed, is developed. To improve the mechanical performance of the continuum arms, additional compliant mechanisms (flexure hinges) were integrated into its design. By combining the dual-arm continuum robot with a commercial unmanned underwater vehicle (UUV), the system can be deployed in many underwater engineering scenarios to conduct complicated tasks. The prototyped dual-arm continuum robot and its control system has been tested to ascertain its kinematic accuracy. It was found the average displacement error is within 5.7% of the 6-DoF continuum robot (length: 540 mm), proving its potential for high-accuracy operation.**

Keywords—continuum robot, robot collaboration, dual-arm robot, material retrieval

I. INTRODUCTION

In many industries worldwide, decommissioning is a significant and growing engineering challenge, especially within the nuclear industry. Indeed, with over 400 civil nuclear reactors in operation globally, 75 percent of which are at least 25 years old, the worldwide nuclear decommissioning market is expected to be worth £250 billion in the decade to 2025 [1]. Nuclear decommissioning activities require the removal of radioactive materials to the point that it no longer requires radiation protection before the progressive demolition of facilities [2, 3]. This is a hazardous, expensive and time-intensive process that is exacerbated when the environment is underwater. However, there is still no suitable manipulator that can cope the aforementioned tasks in the challenging environments.

Currently, a few underwater manipulators are available for use in in-situ environments, but most of them were not designed for the underwater environment or bulky dimension for the confined spaces [4-6]. To perform the high accuracy collaborative operation, the rigid linkage structures were usually adopted [7, 8], which were normally actuated by the heavy-duty actuators (e.g., linear motor units [9], hydraulic cylinders [10] or smart actuators [11, 12]). For example, a kind of new 6-DoF robotic system was built by the rigid linkages [13]. However, the actuators were located in the robot arm, causing the centre of mass (COM) far away from the installation surface. Further, another 7-DoF robotic arm, which is also constructed by the linkage structure, was developed for the underwater environment [14]. But the bulky dimension will stop the combination with the conventional UUV for the confined space operation. Recently, a new kind of continuum robot that actuated by the cable-driven strategy was developed for the confined space operation [15]. However, the stiffness of the system is too low for the desired task. To address the aforementioned challenges, here, a novel dual-arm robot, which is composed of two symmetrical 6-DoF continuum manipulators that are characterized by their compact dimensions, low weight, and dexterous motion capability, has been developed to perform operations in complex underwater environments and remove the limitations with existing manipulators.

The capability of the robotic system to work collaboratively is important for coping with complicated tasks in hazardous/constrained environments [16, 17], as the tasks are often characterized by multistep and multi-target objectives (e.g., sample retrieval from underwater environment: where gripper [18] and grinder [19] end-effectors will be needed). Several collaborative robotic systems and corresponding operation strategies have been developed to successfully cope with in-situ tasks. For example, a dual-arm humanoid robot, which is composed by two 6-DoF arm robots, was developed for the sample preparation and measurement processes [20]. With functional end-effectors, numerous cooperative operations can be achieved. Further, two different continuum arms were working together to enhance the performance of the individual continuum arms, in which the two continuum arms were combined and reconfigured as a parallel manipulator [21]. There are several more cases of miniature robotics (e.g., swarm [22] and crawling [23] robots) cooperatively working together to complete complicated tasks by wireless communication. This comparable with the "army-ant" approach to improve the group capability by using a great number of simple, inexpensive and physically identical robotic units. However, these cooperative

EPSRC of UK (EP/V027379/1)

robotic systems are not suitable for challenging underwater environments.

To overcome these challenges, a new dual-arm robotic system, which is comprised of two 6-DoF continuum robots and corresponding end-effectors, has been developed for coping with engineering tasks in constrained environments. The key features of the system can be summarized as the following: 1) two 6-DoF cable-driven continuum manipulators have been integrated capable of performing cooperatively, reducing weight and improving dexterity; 2) given the manipulators are cable-driven, the electrical hardware can all be placed within a single sealed unit simplifying waterproofing and environmental protection; 3) the dual-arm robotic system can be attached to a commercial ROV system for underwater applications, with the added advantage that the COM of the manipulators is close to constant and near the centre of the ROV, increasing stability and simplifying control.

II. Problem Definition and Solution

In order to perform the nuclear decommissioning from the underwater environment, a new kind of dual-arm robotic system with multiple DoFs, which is combined with the commercial underwater unmanned vehicle for the underwater environment operation, is developed.

A. *Task-oriented design*

Taking the Fukushima Daiichi Nuclear Power Plant (FDNPP) environment as the case study, it is one of the submerged scenarios that needs the repetitive in-situ intervention for the safety decommissioning. In order to check the radioactivity intensity of the damaged FDNPP, the samples need to be retrieved from the in-situ environment, requiring a new underwater robotic system to be developed. Figure 1 (a) shows the real scenario of the damaged FDNPP, where the damaged nuclear reactor is firmly combined with the building structures together, resulting the difficulty to retrieve the fragment from the environment. For this application, the developed robotic system needs to have the following two functions: 1) the material removing tool (e.g., grinder or cutter) is needed to cut the fragment from the environment; 2) the material collecting tool (e.g., gripper or string bag) is needed to collect the removed material.

Based on the aforementioned requirements, a dual-arm robotic system has been developed and combined with a commercial UUV, as seen in Figure 1 (b). One arm has been integrated with a grinder as an end effector to cut the material from the environment, while the other arm has a gripper to collect the removed fragment. The gripper also aids the stability of the overall system during the material removal process, which is required as the reaction force from the grinder will cause the position of the system (i.e., UUV + dual-arm robot) to drift.

For a specific task, the two end-effectors need to work together. Taking the sample retrieval as an example, the system should have the material removal function (e.g., grinding, drilling and laser cutting), and also the collection function for the removed material. Based on the above requirements, the smart grinder and griper were designed and equipped at the tip of the two continuum robots, seen in Figure 1. During the operation, the gripper continuum robot adjusts its configuration (i.e., bending of the three sections) to ensure the correct and firm gripping. Then, the grinder continuum robot runs the planned trajectory to cut the material off from the environment. At last, the UUV system carries the robotic system, as well as the removed material, out of the in-situ environment.

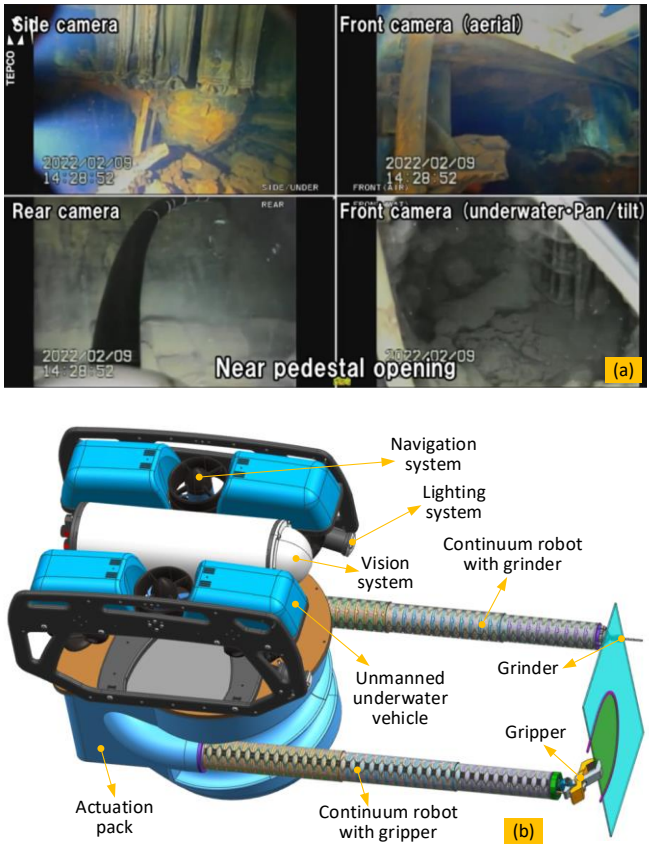

Figure 1 Task-oriented design of the dual-arm robotic system for the underwater sample retrieval: a) is the real scenario of damaged FDNPP; b) is the structure design of the dual-arm robotic system with gripper and grinder at the tip, respectively

B. *Working principle of the continuum robot*

To improve the dexterity and to achieve the 6 degrees of freedom of the end-effector of the dual-arm robotic system, the two arms are designed with a continuum structure. Specifically, each continuum arm is composed of three serially connected 2-DoF cable-driven segments. To actuate the two continuum arms, the cables are tensioned by the motor units located at the actuation pack, seen in Figure 1 (b). This results in the following advantages for the system:

- Dexterous operation: each continuum arm has 6-DoF of motion within a large workspace (shown later).
- Improved stability of the system: the actuation units (e.g., motor units with motor, gear box and encoder) and the corresponding structural components can be located directly beneath the UUV system, minimizing the disturbance of the UUV to manipulator motion.
- Improved environmental protection: as all the actuation units and control hardware is within the actuation pack, protecting them from egress is easier and more robust.

However, adopting the 6-DoF continuum arm brings the following challenges for the high-accuracy control of the system:

- Low stiffness: as the continuum manipulators are slender in design and operated in a cantilever configuration, high deviation from the desired position may be caused by external loads.
- Motion redundancy exists in each 2-DoF continuum arm, resulting in kinematic complexity.
- Low kinematic accuracy: as the continuum arms are constructed by multiple joints, the friction in the joints will affect the kinematic accuracy.

To solve these challenges, a novel attempt has been taken in this paper by integrating compliant structures (character: compact structure and powerful) to the conventional continuum robot (character: high redundancy and modular structure) to improve the mechanical performances (e.g., stiffness, positioning and repeatability accuracies).

To illustrate the concept of the novel compliant hinge-based continuum robot, a typical application of continuum or snake robots (that is, pipe repair), which is very difficult for conventional robots (e.g., 6R arm robot) to access, was selected, as seen in Figure 2. In this scenario, an active three-section continuum robot, in which each section can be independently deployed to achieve the 2-DoF movement, was controlled by the actuation pack to be deeply inserted into the environment, seen in Figure 2 (a). However, to develop this kind of continuum robot with extra high length-diameter ratio, the structure should be carefully designed to guarantee positioning accuracy. One conventional solution (i.e., using compression springs to improve the kinematic accuracy) for the challenge is shown in Figure 2 (b), where the upper and lower platforms are connected by the central ball joint. However, the challenges still existing when these conventional compression springs are used. For example, the conventional compression spring may have a high axial stiffness when it is compressed, but the torsional stiffness is very low and cannot be regulated. This is a problem for the continuum robot with high-accuracy requirement.

To improve the operational accuracy of the 2-DoF mechanism, a class of novel spring concepts, which combined with compliant and soft materials, were developed, as seen in Figure 2 (c) to (f):

1) Diamond-shape leaf, shown in Figure 2 (c): four compliant pivots were adopted in a diamond configuration to achieve the following advantages: firstly, the lower axial compressive stiffness can be obtained, enabling the 2-DoF motion of the parallel mechanism, seen in Figure 2 (b); secondly, the radial stiffness is much higher, enabling the parallel mechanism to have higher rotational stiffness; thirdly, the stiffness of this mechanism can be easily adjusted by changing the thickness of the flexible pivots.

2) Another possible solution is shown as Figure 2 (d) with two arc-shape pivots adopted and symmetrically distributed in left and right. The arc structure of the compliant pivots can support higher axial compressive deformation, as lower material stress is produced when the structure is deformed.

Due to the modular structure of the compliant hinges (i.e., the material for deformation parts and fixture parts are same), they can be replaced by different materials with different mechanical properties (i.e., superelastic NiTi rods in Figure 2 (e) and hyperelasic rubber in Figure 2 (f)). These novel hyperelasic materials can help the system to adapt to different environments. For example, the compliant rod-based structure can be used in applications where higher

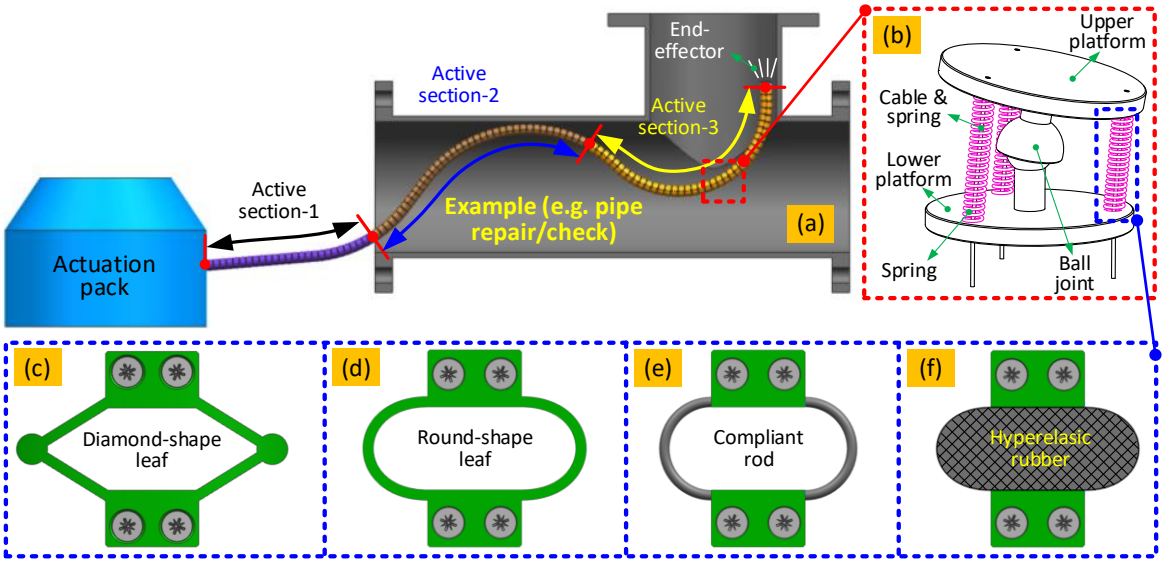

Figure 2.The concept description of the continuum robot that constructed by a class of novel compliant hinges. (a) is an example case study for illustrating the advantages and working principle of conventional continuum robot (i.e., three active sections were equipped) for the pipe replacement and check; (b) is the conventional 2-DoF parallel mechanism (i.e., compressional springs equipped) for constructing the continuum robot; (c) to (f) are the proposed novel compliant hinges-based structures (diamond-shape leaf, round-shape leaf, compliant rod and hyperelasic rubber structures, respectively) for developing the continuum robot with enhanced performance.

deformations and larger induced stresses are requirements for the flexible elements.

In this section, a class of novel structures (i.e., diamond-shape pivot, round-shape pivot, compliant rod and hyperelasic rubber, respectively) were proposed to develop the continuum robots for improving the kinematic accuracy. With these embedded and replaceable compliant structures, the structural properties of the continuum robot can be easily adjusted to adapt to different environments.

III. Modelling of the Dual-Arm Continuum Robot

In this section, we generalized the modelling of the proposed 6-DoF complaint continuum robot (i.e., diamond-shape flexible hinge was selected as the example), which is composed of three 2-DoF continuum sections. With the developed kinematic model, the input-output relationship (i.e., pose of the continuum robot vs length of the driving cables) has been established, which can guide the development of the control system.

A. Coordinate systems and robot kinematics

In this section, a piecewise constant-curvature theory (PCCT) is utilized to describe the 2-DoF spatial motion of each continuum section (i.e., three-sections continuum robot is selected as the example) during the operation of the 6-DoF continuum robot. By regulating the length of the driving cables, the posture and position of the end-effector can be controlled to perform the planned paths for the desired task, which is achieved by the correct kinematic modelling of the 3-section continuum robot.

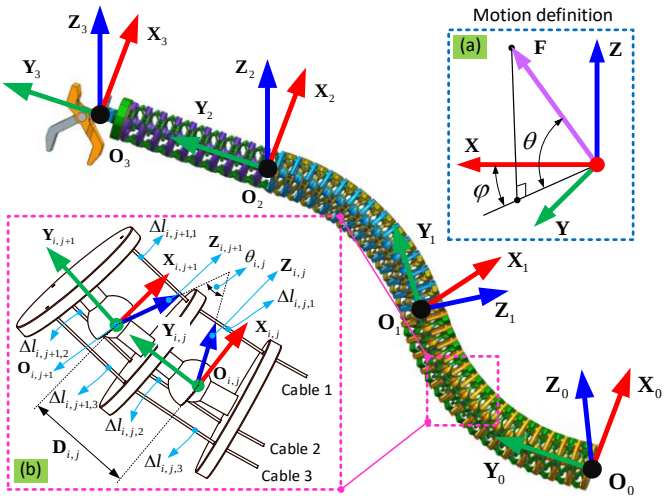

Figure 3. Kinematic sketch of the proposed 6-DoF continuum robot (i.e., three 2-DoF continuum sections were serially connected with the moving coordinate systems): (a) the motion definition for the 6-DoF continuum robot; (b) the kinematic sketch of the example 2-DoF segment

Based on the working principle and structure design of the continuum robot, the three sections are serially connected to achieve the 6-DoF motion of end-effector with enhanced performances (e.g., large workspace and high kinematic accuracy), as seen in Figure 3. Three local coordinate systems ($\{\mathbf{O}_i\}$, i=1,2,3) are attached the base of each 2-DoF continuum section to define the 2-DoF bending motions. One coordinate system $\{\mathbf{O}_3\}$ is attached at the base of end-effector (gripper as the example) to define the position and posture for the task.

Taking a single 2-DoF continuum section as an example, as shown in Figure 3 (b), which consists of a series of identical structured segments. Based on the PCCT, the bending trajectory along its length direction is regarded as in constant-curvature, which means that bending angle for j-th segment in i-th section, θ_{ij}, can be regarded as:

$$\theta_{ij} = \frac{\theta_i}{n} \tag{1}$$

Where, θ_i is the bending angle of i-th continuum section. n is the number of segments of i-th continuum section.

The transformation matrix from $\{\mathbf{O}_{ij}\}$ to $\{\mathbf{O}_{i,j+1}\}$ can be defined as following: first, $\{\mathbf{O}_{ij}\}$ moves from its origin O_{ij} to $O_{i,j+1}$ along the $\mathbf{Z}_{ij}$ axis; then $\{\mathbf{O}_{ij}\}$ rotates around $\mathbf{Y}_{i,j+1}$ axis by angle θ_{ij}. Thus, the homogeneous transformation matrix can be expressed as:

$${}^{O_{i,j}}\mathbf{T}_{O_{i,j+1}} = \begin{bmatrix} \mathbf{R}_{\mathbf{X}}(\theta_{i,j}) & \mathbf{D}_{i,j} \\ 0 & 1 \end{bmatrix} \tag{2}$$

Where $\mathbf{R}_{\mathbf{X}}(\theta_{i,j})$ is the rotation matrix generated by rotating $\mathbf{Y}_{i,j+1}$ axis with angle θ_{ij} of $\{\mathbf{O}_{i,j+1}\}$; $\mathbf{D}_{i,j}$ is the length vector from O_{ij} to $O_{i,j+1}$ of $\{\mathbf{O}_{i,j}\}$.

By post-multiplying the transformation matrix of the three sections, the entire kinematic model of the continuum robot can be established.

$${}^{O_{1,0}}\mathbf{T}_{O_{3,n_3-1}} = \mathbf{T}_0(\varphi) \cdot \prod_{j=0}^{n_1-1} {}^{O_{1,j}}\mathbf{T}_{O_{1,j+1}} \cdot \prod_{j=0}^{n_2-1} {}^{O_{2,j}}\mathbf{T}_{O_{2,j+1}} \cdot \prod_{j=0}^{n_3-1} {}^{O_{3,j}}\mathbf{T}_{O_{3,j+1}} \tag{3}$$

Where n_1, n_2 and n_3 are the number of segments in three continuum sections, respectively; $\mathbf{T}_0(\varphi)$ is the bending direction transformation matrix, which can be written as:

$$\mathbf{T}_0(\varphi) = \begin{bmatrix} \mathbf{R}_{\mathbf{Z}}(\varphi) & \mathbf{0} \\ 0 & 1 \end{bmatrix} \tag{4}$$

In this section, a novel kinematic model was studied for the proposed continuum robots with variable length of the sections, enabling to predict the position and posture of end-effector after providing the phase angle (φ_1, φ_2 and φ_3, respectively) and bending angle (θ_1, θ_2 and θ_3, respectively) of the three sections.

B. Cooperation Workspace Analysis

To improve the functional capability of the robot, two 6-DoF continuum manipulators have been adopted in a manner comparable to human beings, that are equipped with two dexterous arms capable of working collaboratively to complete complicated tasks. The workspace calculation for the single 6-DoF continuum robot is straightforward and can be constructed by adopting the kinematic models developed in last section. However, for the collaborative workspace of the dual-arm continuum robot, it will become complicated as the workspace will not only be dependent on the mechanical characteristics (e.g., bending stroke and length of each 2-DoF segments) of the single 6-DoF continuum robot, but also will be dependent by the

feature of the workpiece (e.g., dimension and shape) and operations.

Based on the kinematic model developed in last section, the workspace of the dual-arm continuum robot can be calculated, which is conducted by plotting the tip position of the two 6-DoF continuum arms when changing the bending and phase angles within their strokes, seen in Figure 4.

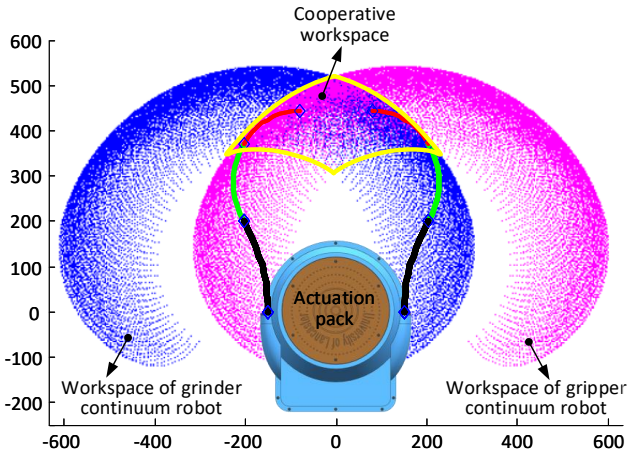

Figure 4. Collaborative workspace of the dual-arm continuum robot. Note: for the better display, the bending ranges for the three sections of the two continuum robots are 30°, 45° and 60° respectively

It can be seen from Figure 4 that the workspace of each 6-DoF continuum robot is a section of a spherical shell, which is caused by the symmetrical design of the continuum robot. In order to achieve the ability to work collaboratively, the two spherical shells should have overlapping volumes, enabling the tip of each 6-DoF continuum robot to arrive at a given point within this volume. The section in blue is the workspace of the grinder continuum arm, while the area in pink colour is the workspace of the continuum arm with the gripper end effector. The overlapping area is in the shape of a cownose ray (yellow curve), which can be used to define for the path plan of the two continuum arms for a given task.

Based on the biomimetic design, the dimensions (e.g., diameter of continuum arm and width of the flexure hinge) in section-1 are designed to be larger than in section-2 and section-3 to improve the kinematic performance of the structure. The detailed structure parameters of the 6-DoF continuum arm can be seen in Table 1.

Table 1. Structure parameters of the continuum robot (unit: mm)

Parameters	Length	Diameter	Width	Thickness
Section-1	210	46	6	1
Section-2	180	43	5	1
Section-3	150	40	4	1

IV. Prototype of the Dual-Arm Continuum Robot

With the help of the kinematic model developed in the previous section, the input-output behavior of the system (e.g., length of the driving cables & shape of the continuum robot, external loads & deviation at the tip) can be obtained theoretically. To confirm the performance of the dual-arm continuum robot, a prototype and control system was built and assessed by a set of experimental tests. Also, the kinematic performance of the continuum robot prototype was tested to demonstrate the advantages of the proposed concept.

A. Physical dual-arm continuum robot

The physical dual-arm continuum robot is shown in Figure 5, which is composed of the two 6-DoF continuum robots, two end-effectors (i.e., gripper and grinder respectively), actuation system (i.e., 18 motors for continuum robots and two motors for the gripper and grinder respectively), hardware for the control system, GUI controller. For controlling the shape of the

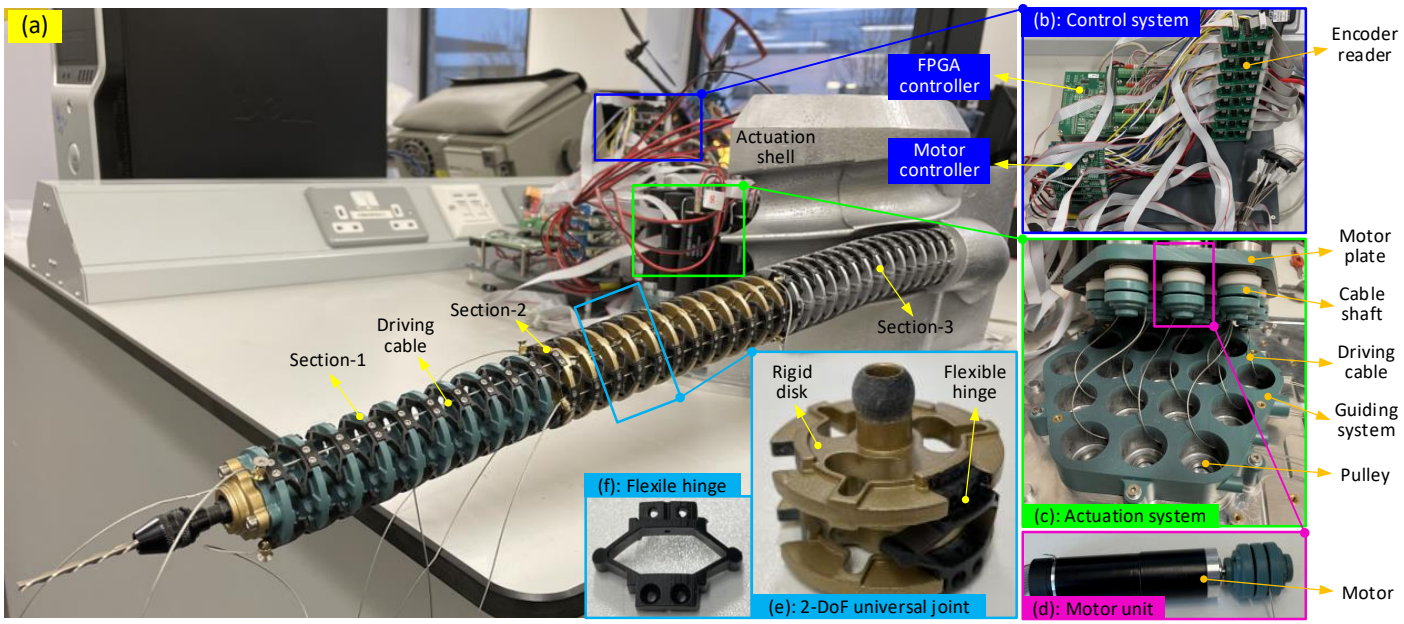

Figure 5. Experimental setup and detailed structure of the continuum robot system: (a) is the overall structure of the system; (b) is the real-time closed-loop control system; (c) is the actuation system for adjusting the length of the driving cables; (d) is the motor unit; (e) is the 2-DoF universal joint; (f) is the flexure hinge

continuum robots and gripping motion of the gripper, displacement-based closed-loop controllers were developed. While for the grinder, a speed-based closed-loop controller was developed. In order to improve the response speed of the system, a National Instruments sbRIO-9627 FPGA-based embedded controller has been used. A GUI was developed using LabView software for regulating the real-time shape of the continuum robots, rotating speed of the grinder and closure of the gripper.

In the actuation system, nineteen Maxon motor units (motor type: RE 25, gearbox: GP26 A with reduction ratio of 236, encoder: ENC16 with 1024 pulses) were compactly arranged. To transfer the power from the motor, flexible steel cables supported by flexible spring tubes with a higher compression stiffness were attached. In addition, the flexible hinges were fabricated to obtain the desired performance (i.e., higher rotational stiffness and low bending stiffness) using additive manufacturing (digital light processing (DLP); machine type: Photocentric LC Magna, resolution: 137 μm, material: durable resin).

B. Kinematic accuracy test of the 6-DoF continuum arm

The experimental setup of the 6-DoF continuum robot is shown in Figure 6. Three 2-DoF sections are serially connected to form the 6-DoF continuum robot. To validate the developed model and test the kinematic accuracy of the continuum robot, grid paper with 2 mm spacing was placed as the background, seen in Figure 6. By adjusting the length of the driving cables by the proposed kinematic model, the shape of the 6-DoF continuum robot can be controlled.

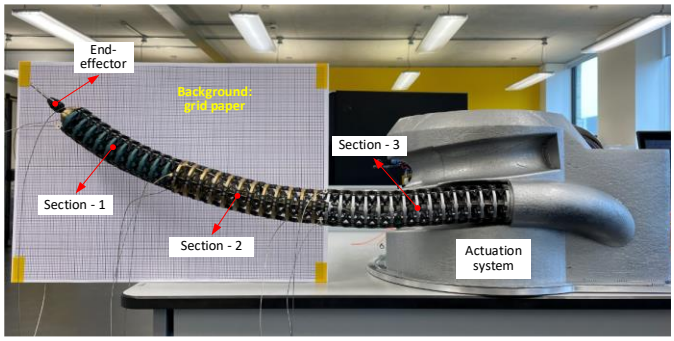

Figure 6. Experimental setup of the 6-DoF continuum robot

Figure 7 shows the comparison between the theoretical calculation and the experimental tests at given set deformations 6-DoF continuum robot. As the workspace of the 6-DoF continuum robot is larger than the size of the grid paper, only the tip two sections (i.e., section 1 and 2) are actuated for the validation, while the base section (i.e., section 3) is kept straight during the test. For the different testing locations, the length of the driving cables were first calculated by the kinematic model and then used by the control system to specify the required rotation of the motors. After the continuum robot arrived at the specified position, a vision-based sensor system captures the position of the continuum robot for the comparison.

It can be seen from Figure 7 that the prototyped 6-DoF continuum robot can achieve a high kinematic accuracy (average error within 5.7%) by using the cable-driven method and embedded flexure hinges. The highest error (about 11.4%) occurs at the beginning of the test when the specified bending angles are small. This is mainly caused by the backlash of the driving cables and internal friction. But, with the increase of the bending angle, the kinematic accuracy is greatly improved (e.g., 4.8% error with the 30° bending angle). The reason for the improved kinematic accuracy is that the tension of the driving cables removes any slack in the system, thus the effects of elongation and friction of the driving cables on the kinematic accuracy will be decreased, resulting the higher accuracy. This is a common phenomenon in continuum robot control, especially when the continuum robot is constructed with multiple sections. To solve this problem, we will develop a new tension regulation algorithm for actively adjusting the tension of the driving cables.

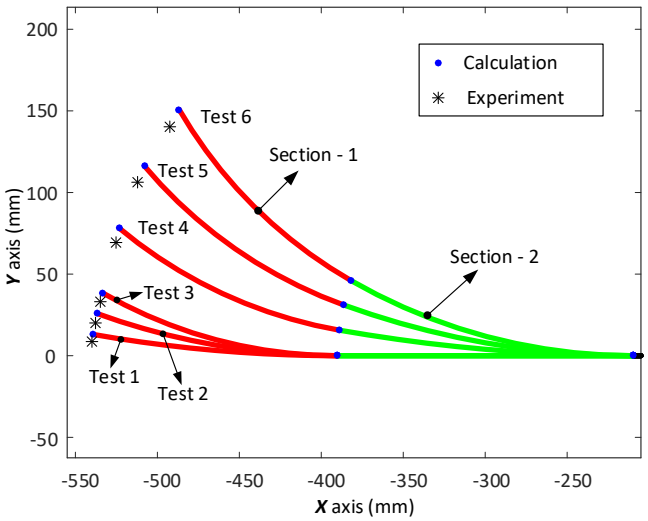

Figure 7. Validation result of the kinematic model between the experimental test and theoretical calculation on the developed prototype

V. CONCLUSIONS

In this paper, a novel dual-arm continuum robot, which is composed by two 6-DoF continuum arms, is developed for collaborative operation in complex and constrained environments. Further, by combining the developed dual-arm continuum robot with a commercial ROV manipulator, the wider application (e.g., underwater engineering or decommissioning) can be demonstrated.

The first trial of integrating compliant mechanisms into the continuum robot to improve the kinematic performance has been shown in this paper. Specifically, diamond-shaped flexure hinges have been integrated with a three-section ball joint-based continuum arm. By combining two 6-DoF continuum robots on the same actuation pack, collaborative operations can be achieved for complicated tasks (e.g., sample retrieval from the underwater environment in this paper). With the prototyped dual-arm continuum robot and control system, this collaborative operation is a promising way to tackle complicated tasks that are hard/impossible for the conventional robots (e.g., parallel or arm robots).

In the next stage, the developed dual-arm robotic system will be mounted with a commercial ROV for the real challenging environments. Further, the advanced control algorithm with the

consideration of the deformation of the continuum arm and loads of the end-effectors will be developed to improve the working performance.

ACKNOWLEDGMENT

This research was funded by the EPSRC through the ASUNDER project (EP/V027379/1).

REFERENCES

[1] M. Laraia, "Nuclear decommissioning," Planning, Execution and International, 2012.

[2] C. J. Taylor and D. Robertson, "State-dependent control of a hydraulically actuated nuclear decommissioning robot," Control Eng. Pract., vol. 21, no. 12, pp. 1716-1725, 2013.

[3] N. Marturi et al., "Towards advanced robotic manipulation for nuclear decommissioning: A pilot study on tele-operation and autonomy," in. IEEE, 2016, pp. 1-8.

[4] Y. Wang, S. Wang, Q. Wei, M. Tan, C. Zhou, and J. Yu, "Development of an underwater manipulator and its free-floating autonomous operation," IEEE/ASME Transactions on Mechatronics, vol. 21, no. 2, pp. 815-824, 2015.

[5] T. W. Mclain and S. M. Rock, "Experiments in the hydrodynamic modeling of an underwater manipulator," in. IEEE, 1996, pp. 463-469.

[6] K. Ioi and K. Itoh, "Modelling and simulation of an underwater manipulator," Adv. Robotics, vol. 4, no. 4, pp. 303-317, 1989.

[7] S. Hachicha, C. Zaoui, H. Dallagi, S. Nejim, and A. Maalej, "Innovative design of an underwater cleaning robot with a two arm manipulator for hull cleaning," Ocean Eng., vol. 181, pp. 303-313, 2019.

[8] V. Kramar, A. Kabanov, O. Kramar, and A. Putin, "Modeling and testing of control system for an underwater dual-arm robot," in. IOP Publishing, 2020, p. 42076.

[9] N. Ma, X. Dong, and D. Axinte, "Modeling and experimental validation of a compliant underactuated parallel kinematic manipulator," IEEE/ASME Transactions on Mechatronics, vol. 25, no. 3, pp. 1409-1421, 2020.

[10] C. Kim, T. Kim, and M. Lee, "Study on the estimation of the cylinder displacement of an underwater robot for harbor construction using a pressure sensor," Journal of Navigation and Port Research, vol. 36, no. 10, pp. 865-871, 2012.

[11] N. Ma, X. Dong, J. C. Arreguin, C. Bishop, and D. Axinte, "A class of novel underactuated positioning systems for actuating/configuring the parallel manipulators," Robotica, pp. 1-20, 2022.

[12] N. Ma, X. Dong, J. C. Arreguin, and M. Wang, "A novel shape memory alloy (SMA) wire-based clutch design and performance test," in. Springer, 2020, pp. 369-376.

[13] H. Yin, S. Huang, M. He, and J. Li, "A unified design for lightweight robotic arms based on unified description of structure and drive trains," International Journal of Advanced Robotic Systems, vol. 14, no. 4, p. 1734873759, 2017.

[14] J. Koch et al., "Development of a robotic limb for underwater mobile manipulation," in. IEEE, 2018, pp. 1-5.

[15] Ma, Nan. "Design and modelling of a continuum robot with soft stiffness-adjustable elements for confined environments." (2022).

[16] N. Ma, X. Dong, J. C. Arreguin, C. Bishop, and D. Axinte, "A class of novel underactuated positioning systems for actuating/configuring the parallel manipulators," Robotica, pp. 1-20, 2022.

[17] J. Tao and D. Li, "Cooperative strategy learning in multi-agent environment with continuous state space," in. IEEE, 2006, pp. 2107-2111.

[18] H. Zhou and N. Ma, "Modeling and experimental implementation of a flexible SMA wire-based gripper for confined space operation," J. Intel. Mat. Syst. Str., pp. 1045389X-221077428X, 2022.

[19] P. Hamelin, P. Bigras, J. Beaudry, P. Richard, and M. Blain, "Discrete-time state feedback with velocity estimation using a dual observer: application to an underwater direct-drive grinding robot," IEEE/ASME Transactions on Mechatronics, vol. 17, no. 1, pp. 187-191, 2011.

[20] H. Fleischer et al., "Application of a dual-arm robot in complex sample preparation and measurement processes," Journal of laboratory automation, vol. 21, no. 5, pp. 671-681, 2016.

[21] M. Russo, N. Sriratanasak, W. Ba, X. Dong, A. Mohammad, and D. Axinte, "Cooperative continuum robots: Enhancing individual continuum arms by reconfiguring into a parallel manipulator," IEEE Robotics and Automation Letters, vol. 7, no. 2, pp. 1558-1565, 2021.

[22] P. Schleer, S. Drobinsky, M. de la Fuente, and K. Radermacher, "Toward versatile cooperative surgical robotics: a review and future challenges," Int. J. Comput. Ass. Rad., vol. 14, no. 10, pp. 1673-1686, 2019.

[23] J. S. Bay, "Design of the" army-ant" cooperative lifting robot," IEEE Robotics \& Automation Magazine, vol. 2, no. 1, pp. 36-43, 1995.